JOURNAL
OF THE AMERICAN CHEMICAL SOCIETY

VOLUME 98, NUMBER 22 OCTOBER 27, 1976

Comparison of Trajectory Calculations, Transition State Theory, Quantum Mechanical Reaction Probabilities, and Rate Constants for the Collinear Reaction $H + Cl_2 \rightarrow HCl + Cl$

Donald G. Truhlar,*[1a] Jean A. Merrick,[1b] and James W. Duff[1c]

Contribution from Chemical Dynamics Laboratory, Department of Chemistry, University of Minnesota, Minneapolis, Minnesota 55455. *Received February 5, 1976*

Abstract: Quantum mechanical rate constants are computed for the collinear reaction $H + Cl_2 \rightarrow HCl + Cl$ using the reaction probabilities of Baer. For comparison we also computed reaction probabilities and rate constants for this reaction using (a) the quasiclassical trajectory method, (b) the reverse quasiclassical trajectory method, (c) the classical S matrix theory (using real-valued trajectories only), and (d) transition-state theory assuming separability of the reaction coordinate at the transition state. Comparisons are made not only for total reaction probability and total rate constant but also in general for state-to-state reaction probabilities and state-to-state rate constants. The quasiclassical trajectory method is generally accurate except in the threshold regions for various state-to-state processes. It is more accurate for total reaction probabilities and total rate constants than for state-to-state reaction probabilities and rate constants. The quasiclassical trajectory calculations of total rate constants for reaction in a given initial vibrational state agree with the quantum calculations within 29% for the 300-1000 K temperature range but the state-to-state rate constants may be in error by a factor of 2 or more even for processes which are classically allowed in the sense of classical S matrix theory. Classical S matrix theory does not always provide a more accurate way to extract state-to-state reaction probabilities from these trajectories. Transition state theory (which yields average reaction probabilities and total rate constants for a thermal distribution of initial states but does not yield state-to-state results) is fairly accurate for this reaction even with the assumption that the reaction coordinate is separable.

I. Introduction

Molecular trajectory calculations[2] are an important and useful method for studying cross sections, rate constants, and product energy distributions for gas-phase chemical reactions. A popular type of trajectory calculation is the quasiclassical trajectory method.[3] In this method analysis of final classical energy distributions in terms of quantum states of the product is usually performed using the histogram method.[4] The quasiclassical trajectory method is inaccurate in general due to lack of knowledge of the correct potential energy surface, to statistical errors when enough trajectories are not run, and to the inadequacy of classical mechanics for certain aspects of chemical dynamics. The last of these sources of error is poorly understood. In principle it is straightforward to study this source of error: one assumes a realistic potential energy surface, calculates exact quantum mechanical cross sections and rate constants, and compares these to quasiclassical cross sections and rate constants computed with a small enough statistical error for the same potential energy surface. Since calculation of exact quantum mechanical cross sections has just become practical and since exact quantum mechanical rate constants have not yet been published, such comparisons have been limited to cross sections for three-dimensional[5] and planar[6] $H + H_2$ and to collinear reactions.

Comparisons of exact-quantum and quasiclassical-trajectory collinear reaction probabilities have been presented for the thermoneutral reaction $H + H_2$,[7-14] the slightly endothermic reaction $Cl + H_2$ and its isotopic analogues,[15] and the exothermic reactions $F + H_2$,[16-18] $F + D_2$,[19,20] and $H + Cl_2$.[21] However, Baer[22] has concluded that the quantum calculations used for the last-named comparison seem to be inaccurate. Comparisons of exact quantum and quasiclassical trajectory calculations on the level of one-dimensional rate constants are even more scarce and such comparisons have been presented only for $Cl + H_2$, $F + H_2$, and some of their isotopic analogues.[15,18,19] In this article we compare Baer's accurate quantum reaction probabilities for $H + Cl_2$ to the results of newly computed quasiclassical trajectory calculations. Further we compute one-dimensional rate constants from both sets of reaction probabilities and we compare these. Our comparison includes rate constants for reactions of vibrationally excited reagents, a feature not present in any previous comparisons.

Another method of calculating reaction probabilities, cross sections, and rate constants from classical trajectories is the

classical S matrix theory.[23] In general classical S matrix theory involves contributions from both complex-valued and real-valued trajectories. Processes for which the latter contribute in a stationary phase approximation are called classically allowed.[20,23,24] In this article we compare exact quantum collinear reaction probabilities and one-dimensional rate constants to classical S matrix calculations involving real-valued trajectories only. The motivation for restricting ourselves to real-valued trajectories is to test the two most general methods (quasiclassical trajectory method and classical S matrix theory for classically allowed processes) for using real-valued classical trajectories to study chemical reaction cross sections and rates. The use of complex-valued trajectories is more difficult and is not a widely used technique for studying chemical reactions; complex-valued trajectories have been calculated for reactive collisions in only a few cases[20,24] and in one case[18] a simpler analytic continuation technique was used. The complex-trajectory technique has not been demonstrated to be a generally practical method for treating reactive collisions. Classical S matrix theory collinear reaction probabilities and one-dimensional rate constants have previously been compared to accurate quantum results only for H + H_2,[10-13,14b,25] F + H_2,[17,18] and F + D_2.[19,20] Miller and Rankin[26] calculated a few state-to-state reaction probabilities for H + Cl_2 using classical S matrix theory and the quasiclassical trajectory histogram method, but they indicated that a detailed comparison with accurate quantum results was not possible because the quantum results then available neglected closed channels and used a harmonic approximation. Baer[22] has also found those quantum results to be inaccurate. A comparison of quantum and classical S matrix results for planar H + H_2 has also been reported.[6]

What has been learned from the previous tests of real-valued trajectory methods against exact quantum results for non-thermoneutral reactions?[14b] Baer, Halavee, and Persky[15] found the quasiclassical trajectory technique underestimated the total reaction probabilities for Cl + H_2 and three of its isotopic analogues for ground-state reactants near threshold but for Cl + HD → HCl + D it overestimated the reaction probability for ground-state reactants near threshold except in the very low energy region which is classically forbidden. At higher relative kinetic energies, up to about 14 kcal/mol, the trajectory results for total reaction probabilities for ground- or excited-state reactants agreed with the quantum results on the average although they showed no oscillations. The deviations were larger for excited-state reactants and this was attributed to the greater role of resonances in that case. The deviations were also larger for state-to-state reaction probabilities than for total reaction probabilities. Baer et al. found that rate constants computed from the trajectories differed from accurate quantum ones by factors of 0.63 to 2.34 at 300 K but only 0.86 to 1.81 at 1000 K. Transition-state theory was only slightly less accurate than the trajectory method for computing rate constants. For the exothermic F + H_2 and F + D_2 reactions, Schatz, Bowman, and Kuppermann[17-19] and Whitlock and Muckerman[20] found that quasiclassical trajectory calculations and uniform classical S matrix calculations generally gave similar results for the classically allowed transitions. The main exception was the transition probability for producing the most highly excited energetically allowed product state. For this state the quasiclassical trajectory histogram method predicted too high a threshold but uniform semiclassical and reverse quasiclassical calculations were more accurate. For F + H_2 the uniform semiclassical method was more accurate than the reverse quasiclassical method but the opposite was true for F + D_2.[18,19] But the reverse quasiclassical method predicted an incorrect reaction threshold of zero relative translational energy. The fraction of available energy appearing as product vibration was correct within about 10% at given energies but was not averaged over thermal distributions of relative translational energy. Thermally averaged ground-state-to-product-state rate constants were much more accurate at 1000 than 300 K. No previous tests of trajectory methods for excited-state reactants are available for exothermic reactions.

The H + Cl_2 reaction has been extensively studied both experimentally and theoretically.[27] However, many of the conclusions of the present study should apply not only to this important reaction but also to other similar reactions, especially exothermic reactions of a light atom with a heavy molecule. For this mass combination, many aspects of the collinear reaction are reasonably representative of the reaction in a larger number of dimensions,[28,29] at least when the potential energy surface favors collinear reaction. The potential energy surface for the real H + Cl_2 system is believed to favor collinear reaction[30] and the approximate H + Cl_2 potential energy surface used for the present study also favors collinear reactions.

II. Calculations

A. Potential Energy Surface. The potential energy surface used for these calculations, and Baer's accurate quantum calculations to which comparison is made, is a LEPS semiempirical surface whose parameters are given by Baer.[22] For this surface the classical exothermicity is 48.64 kcal/mol. We calculated a classical barrier height E_b of 2.42 kcal/mol and saddle point coordinates of 2.017 Å for the Cl–Cl distance and 2.251 Å for the H–Cl distance (which may be compared to reagent equilibrium internuclear distance of 2.000 Å and product equilibrium internuclear separation of 1.273 Å, respectively).

B. Reagent and Product Vibrational States. All energies will be measured from the classical potential energy minimum for the H + Cl_2 reagent. We used masses of 1.008 amu for H and 35.5 amu for Cl. The usual expression for the eigenenergies of a Morse oscillator and the parameters used for the potential energy surface then yield the energies for the asymptotic quantized vibrational states given in Table I. These agree with the values given by Baer within 0.04 kcal/mol for Cl_2 but much more poorly for HCl, presumably due to inaccuracies in the quantum calculations. (Using a mass of 35 amu for Cl does not change the comparison appreciably.) Hopefully any associated inaccuracies in the quantum probability calculations do not affect the major conclusions of the comparison of dynamical quantities in this article.

C. Trajectories. The trajectories were calculated using a modified version of a program described elsewhere.[13] The following parameters for the numerical integration were found to lead to suitably accurate results: initial and final R_{HB} (the Cl atoms are labeled B and C, respectively, and the internuclear distances satisfy $R_{HC} = R_{HB} + R_{BC}$) equal to 5.5 Å, final R_{BC} equal to 5.0 Å, and time step equal to 2×10^{-16} s. Many trajectories were back-integrated to test their accuracy.

From the results of the quasiclassical trajectories[31] we calculate the reactive transition probabilities $P_{n_1n_2}^{R}$ for H + $Cl_2(n_1)$ → $HCl(n_2)$ + Cl, where n_1 and n_2 are vibrational quantum numbers, using classical S matrix theory in its various orders of approximation and using the quasiclassical trajectory histogram method. The classical S matrix methods have been adequately discussed, with references, elsewhere[13,23,24,32,33] and so we will not repeat all the details. The orders of approximation we investigated are the classical limit (CSC), the primitive semiclassical (PSC), the Airy uniform semiclassical (AUSC), and the Bessel uniform semiclassical (BUSC) approximations. The formulas for these approximations (CSC,[13,32] PSC,[13,32] AUSC,[13,32] and BUSC[33]) are given elsewhere. Henceforth we add the suffix CA to these abbreviations to serve as a reminder that only real-valued trajectories

Table I. Eigenstates E_n^v of Cl_2 and HCl (kcal/mol)

n	Cl_2	HCl
0	0.79	−44.40
1	2.37	−36.19
2	3.92	−28.31
3	5.45	−20.78
4	6.95	−13.60
5	8.44	−6.76
6	9.90	−0.26
7	11.34	5.90
8	12.76	11.71

(classically allowed processes) are included in the present study of these semiclassical approximations. To evaluate $P_{n_1n_2}^R$ in these semiclassical approximations we located the roots of $n_2(\bar{q}_1,n_1) = n_2$ [where, in the notation established previously,[13,32] $n_2(\bar{q}_1,n_1)$ is the final vibrational action as a function of initial vibrational phase shift $\bar{q}_1$ and quantum number n_1; n_2 is the integer in $P_{n_1n_2}^R$] between two trajectories differing in $\bar{q}_1$ by $2\pi/210$ or $2\pi/420$ [the latter was necessary to obtain accurate values for the phase $\phi(\bar{q}_1,n_1)$ of the classical **S** matrix accurately at energies very near a threshold for a given state-to-state process to become classically allowed], and obtained the necessary information corresponding to the root by an interpolation procedure described previously.[34] In all cases considered here, when the quasiclassical probability of reaction ${}^{QC}P_{n_i}^R$ is unity (total energies 3.46–9.22 kcal/mol for $n_1 = 0$ and 5.26–7.40 kcal/mol for $n_1 = 1$) there are zero or two roots for each given state-to-state process but when ${}^{QC}P_{n_1}^R$ is less than unity (other energies for $n_1 \leq 1$ and all energies for $n_1 = 2$) there are zero or more than two roots. In the latter cases we included only the two roots with largest values of the Jacobian $[2\pi\ \partial n_2(\bar{q}_1,n_1)/\partial\bar{q}_1]^{-1}$. In favorable cases the other roots could be treated using a statistical approximation.[26] However, it is often difficult to decide whether a given root trajectory is part of a statistical region. This is illustrated by the trajectory functions plotted in Figure 1. The trajectory functions are shown for n_1 equal 0 in the energy range 3.025–3.69 kcal/mol, which is the region just above the threshold for reaction. Consider, for the first example, the calculation of P_{03}^R. At E equals 3.15 kcal/mol, the trajectories with Jacobians of 0.151 and 0.267 have collision lifetimes Q_{cl} (as defined previously[13]) of -7.2×10^{-14} and -8.1×10^{-14} s, respectively, while the root trajectories with Jacobians of 0.077 and 0.005 have Q_{cl} equal to -7.9×10^{-14} and -5.0×10^{-14} s. If one follows these root trajectories as continuous functions of energy the two trajectories with largest Jacobians at 3.15 kcal/mol correlate with the trajectories with Jacobians of 0.042 ($Q_{cl} = -6.3 \times 10^{-14}$ s) and 0.156 ($Q_{cl} = -8.5 \times 10^{-14}$ s), respectively, at E equal to 3.229 kcal/mol. But the trajectory with the third largest Jacobian of 0.077 at 3.15 kcal/mol correlates with the trajectory with a Jacobian of 0.078 ($Q_{cl} = -8.1 \times 10^{-14}$ s) at 3.229 kcal/mol. Thus the most direct trajectories (by the criterion of largest Jacobians) at one energy do not correlate with the most direct trajectories at a nearby energy. A similar phenomenon occurs in trying to uniquely define the most direct trajectories as continuous functions of energy for the calculation of P_{04}^R (compare, e.g., the Jacobians of the root trajectories for this process at energies of 3.05 and 3.15 kcal/mol). Schatz et al.[18] found a similar problem for one transition for $F + H_2$ near threshold and for one transition for $F + D_2$ near threshold. They said that the difficulty was alleviated by considering the calculation of the classical **S** matrix theory results from reverse quasiclassical trajectories. However, the trajectory functions for the reverse quasiclassical trajectories beginning with n(HCl) equal to 3 or 4 have the approximate shape of the trajectory functions plotted for the forward direction at 3.05 kcal/mol in Figure 1 and are not simpler. Further using the reverse trajectories does not change the correlation of root trajectories as a function of energy. However, we found it was difficult to decide which root trajectories are most important only for P_{03}^R and P_{04}^R near their thresholds. At higher energies and for other transitions this was not a serious problem. Further it has recently been pointed out that the statistical approximation is not always valid whenever $n_2(\bar{q}_1,n_1)$ is a rapidly varying function of $\bar{q}_1$.[35] For these reasons, and because it is difficult[36-38] to treat three or more root trajectories including those with small Jacobians in a uniform fashion, we included only the two roots with largest Jacobians and we did not take any account of other roots or statistical

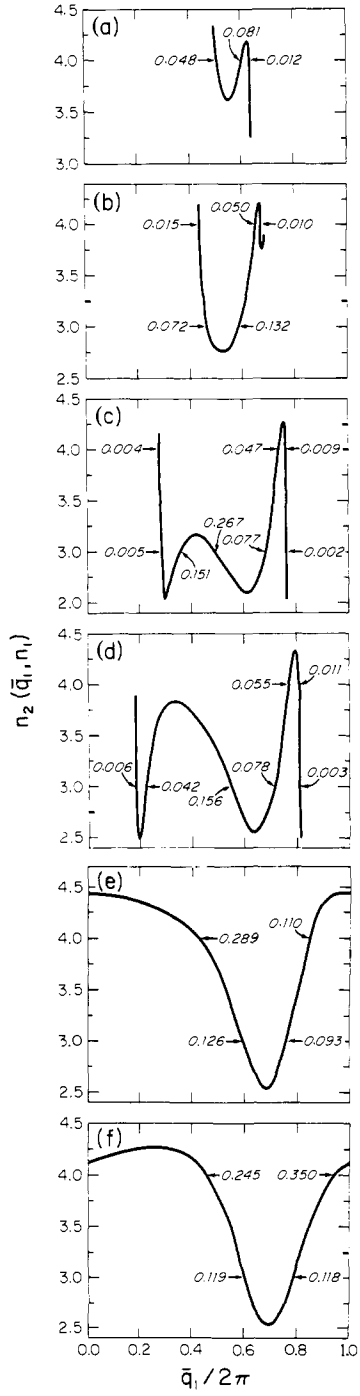

Figure 1. Trajectory functions $n_2(\bar{q}_1,n_1)$ as functions of $\bar{q}_1$ for $H + Cl_2$ ($n_1 = 0$) → HCl + Cl at total energies (a) 3.025 kcal/mol, (b) 3.050 kcal/mol, (c) 3.150 kcal/mol, (d) 3.229 kcal/mol, (e) 3.459 kcal/mol, and (f) 3.690 kcal/mol. The Jacobians $[2\pi(\partial n_2/\partial\bar{q}_1)]^{-1}$ for the root trajectories are given in the figure with arrows pointing to the roots.

contributions. Such corrections would presumably generally be small.

We computed the total reaction probability ${}^{\mathrm{BUSCCA}}P_{n_1}{}^{\mathrm{R}}$ for state n_1 in the BUSCCA approximation by

$$P_{n_1}{}^{\mathrm{R}} = \sum_{n_2} P_{n_1 n_2}{}^{\mathrm{R}} \tag{1}$$

For a given n_1 and a total energy E we first ran 42 trajectories evenly spaced in $\bar{q}_1$. These provided an initial estimate of the $\bar{q}_1$ for each root trajectory and an initial estimate of the $\bar{q}_1$ values which divide reactive from nonreactive regions. These trajectories were also used to compute state-to-state transition probabilities by the forward quasiclassical trajectory histogram method (QCTH method). For the latter purpose, when the total quasiclassical reaction probability was less than unity, we calculated additional trajectories near the boundaries between reactive and nonreactive regions to determine the vibrational phase shift $\bar{q}_1$ at the boundary to an accuracy of $2\pi/210$. We also plotted $n_2(\bar{q}_1)$ and graphically determined the values of $\bar{q}_1$ at which it equals 0.5, 1.5, etc. From these values and from the additional trajectories at the boundaries of the reactive region we found the interval size $\Delta\bar{q}_1(n_2,n_1,i)$ for each interval i where the final vibrational action is closer to n_2 than to any other integer. Then

$${}^{\mathrm{QCTH}}P_{n_1 n_2}{}^{\mathrm{R}} = (2\pi)^{-1} \sum_i \Delta\bar{q}_1(n_2,n_1,i) \tag{2}$$

and ${}^{\mathrm{QCTH}}P_{n_1}{}^{\mathrm{R}}$ was found using eq 1.

In some cases quasiclassical trajectories were run for the reverse (endothermic) direction in order to calculate state-to-state transition probabilities in the exothermic direction by the reverse quasiclassical trajectory histogram (QCTRH) method.[11,17-19,34] The numerical details were the same as for the forward method.

D. Rate Constants. One-dimensional state-to-state rate constants $k_{n_1 n_2}(T)$ were calculated from the reaction probabilities using[39]

$$k_{n_1 n_2}(T) = (2\pi\mu kT)^{-1/2} \times \int_0^{E_{n_1 n_2}{}^{\mathrm{upp}}} P_{n_1 n_2}{}^{\mathrm{R}}(E_{\mathrm{rel}}) e^{-E_{\mathrm{rel}}/kT}\, \mathrm{d}E_{\mathrm{rel}} \tag{3}$$

where μ is the reduced mass and E_{rel} the energy for relative translational motion. $E_{n_1 n_2}{}^{\mathrm{upp}}$ is a number which was taken large enough that $k_{n_1 n_2}(T)$ would not be changed at least to three significant figures, if it were further increased. The integral 2 was evaluated by the trapezoidal rule with a step size of 0.03 kcal/mol for the temperature range 300 K $\leq T \leq$ 1000 K. To obtain the integrand at these grid points we used three-point interpolation (and near threshold for the trajectory calculations, extrapolation) of the integrand with special extrapolation procedures (see below) for the quantum calculations at the lowest energies. We first calculated trajectories in the total energy range E = 2–10.38 kcal/mol with n_1 equals 0, 1, and 2 with most runs being at the same total energies as considered by Baer.[22] Additional trajectories were run to minimize extrapolation errors in the threshold region and to eliminate the need for extrapolation at higher energies and in a few cases at intermediate energies to minimize interpolation errors if our error estimate exceeded 20%. We next summarize the extra trajectory calculations required near threshold and at high energy and the extrapolation procedures used for the quantum calculations.

For the QCTH calculations we were concerned with all transitions connecting the states n_1 = 0, 1, 2 to n_2 = 2, 3, 4, 5, 6. We found ${}^{\mathrm{QCTH}}P_{17}{}^{\mathrm{R}}$ was nonzero for $E \geq$ 8.49 kcal/mol, ${}^{\mathrm{QCTH}}P_{27}{}^{\mathrm{R}}$ was nonzero for $E \geq$ 9.22 kcal/mol, and $P_{07}{}^{\mathrm{R}}$ was nonzero at even higher energy, but the other transition probabilities not considered here had ${}^{\mathrm{QCTH}}P_{n_1 n_2}{}^{\mathrm{R}}$ equal to zero. We calculated enough trajectories near threshold so that the difference between the lowest energy where ${}^{\mathrm{QCTH}}P_{n_1 n_2}{}^{\mathrm{R}}$ was found to be nonzero and the highest energy where it was found to be zero was in the range 0.025–0.3 kcal/mol, typically 0.03–0.05 kcal/mol. In this way we ensured that this region never contributed more than 3% of the total value of the state-to-state rate integral. We found that ${}^{\mathrm{QCTH}}P_{02}{}^{\mathrm{R}}$ becomes zero when E is increased to 5.54 kcal/mol, that the rate integral involving ${}^{\mathrm{QCTH}}P_{03}{}^{\mathrm{R}}$ had converged already at E equals 10.38 kcal/mol, but that for other runs with n_1 equals 0, 1, and 2 $E_{n_1 n_2}{}^{\mathrm{upp}}$ had to be in the range 12–20 kcal/mol.

For QCTRH calculations we considered only trajectories with n(HCl) equals 4 for E in the range 2.54–4.50 kcal/mol, n(HCl) equals 3 for 2.40–4.50 kcal/mol, and n(HCl) equals 2 for 4.15–5.50 kcal/mol. These regions include in each case the threshold energy for the reverse reaction [HCl(n) + Cl → H + Cl_2]. The cases n(HCl) equals 3 and 4 produced $n(Cl_2)$ equals both 0 and 1 and the case n(HCl) equals 2 produced only $n(Cl_2)$ equals 1. In each case, however, $n(Cl_2)$ equals 1 was produced only at the highest energy considered. To calculate state-to-state rates in the forward direction for ground-state Cl_2 we augmented these values at higher energies with QCTH reaction probabilities. The two methods agree better at high energy than low energy and we just attempted to study the large differences closer to threshold.

In the classical **S** matrix calculations we considered the transitions n_1 = 0 to n_2 = 3, 4, 5, 6 and n_1 = 1, 2 to n_2 = 2, 3, 4, 5, and 6. Production of $n_2 \leq 2$ or $n_2 \geq 7$ is classically forbidden (i.e., is not classically allowed) for n_1 = 0 and production of $n_2 \leq 1$ or $n_2 \geq 7$ is classically forbidden for n_1 = 1, 2 for energies $E \leq$ 10.38 kcal/mol. We calculated enough trajectories near threshold so that the difference between the lowest energy at which a state-to-state process was found to be classically allowed and the highest energy at which it was found to be classically forbidden was in the range 0.025–0.284 kcal/mol and was 0.11 kcal/mol on the average. This ensured that the contributions of this energy range to the state-to-state rate integrals was 0.2–20% in each case, averaging 7%. Additional high-energy calculations were performed at E equal to 12, 13, 15, 17, and 20 kcal/mol in some cases.

The quantum probabilities were obtained from the published figures[22] for n_1 = 0, 1 and in numerical form from Baer[40] for n_1 = 2. The threshold regions were found to contribute significantly to the quantum rates but exact probabilities at threshold were not available. Therefore log $P_{n_1 n_2}{}^{\mathrm{R}}$ was extrapolated linearly to E_{rel} = 0 for the rate calculation. In some cases this may overestimate the rate; an approximate estimate of the possible error due to this extrapolation was obtained by also calculating the rates with $P_{n_1 n_2}{}^{\mathrm{R}}$ extrapolated linearly to zero in the threshold region. The latter procedure probably underestimates the contribution of the threshold region to the rate. The contributon to the state-to-state rate from the extrapolated region ranged from 1 to 92% and averaged 28% for the logarithmic extrapolation and ranged from 1% to 65% averaged 12% for the linear extrapolation. High-energy reaction probabilities (energies greater than 10.38 kcal/mol for n_1 = 0, 1 and greater than 12 kcal/mol for n_1 = 2) needed for the quantum rate calculations were assumed equal to those obtained in the QCTH and BUSCCA calculations, whichever agreed best with the quantum results at the highest energy for which the quantum results were available.

In addition to the state-to-state rate constants $k_{n_1 n_2}(T)$ we also computed the rate constants for the reaction out of a given initial state defined either as

$$k_{n_1}(T) = \sum_{n_2} k_{n_1 n_2}(T) \tag{4}$$

Table II. The Fraction of Energy $f_{n_1}(T)$ in Product Vibration for Reactant in the Initial State with Quantum Number n_1

T, °K	n_1	$f_{n_1}(T)$ Quantum	QCTH	BUSCCA
300	0	0.58	0.58	0.58
400		0.58	0.58	0.58
600		0.59	0.58	0.58
1000		0.59	0.58	0.58
300	1	0.58	0.65	0.67
400		0.62	0.65	0.67
600		0.64	0.65	0.66
1000		0.64	0.63	0.65
300	2	0.69	0.73	0.63
400		0.70	0.73	0.64
600		0.70	0.71	0.65
1000		0.68	0.68	0.64

or as

$$k_{n_1}(T) = (2\pi\mu kT)^{-1/2} \times \int_0^{E_{n_1}^{upp}} P_{n_1}^{R}(E_{rel}) e^{-E_{rel}/kT}\, dE_{rel} \quad (5)$$

where $E_{n_1}^{upp}$ is 13–15 kcal/mol for $n_1 = 0$, 15 kcal/mol for $n_1 = 1$, and 18–19.5 kcal/mol for $n_1 = 2$. We also computed the thermally averaged rate constants for production of specific final states as

$$k^{n_2}(T) = \sum_{n_1} P_{n_1}(T) k_{n_1 n_2}(T) \quad (6)$$

where $P_{n_1}(T)$ is the probability of an initial vibrational state and is given by

$$P_{n_1}(T) = (Q^v)^{-1} \exp[-(E_{n_1}^v - E_0^v)/kT] \quad (7)$$

where Q^v is the vibrational partition function and $E_{n_1}^v$ is one of the initial vibrational energies of Cl_2 given in Table I. Finally we computed the thermal rate constant which may be defined either as

$$k(T) = \sum_{n_1} P_{n_1}(T) k_{n_1}(T) \quad (8)$$

or as

$$k(T) = \sum_{n_2} k^{n_2}(T) \quad (9)$$

For each rate constant at each temperature estimates of the possible numerical errors in the QCTH, QCTRH, and BUSCCA results were obtained by comparing the results obtained using the three-point interpolations and extrapolations (preferred method) to those obtained using two-point linear and two-point and three-point logarithmic interpolations and extrapolations to calculate the rate constants. The error estimates we give are in each case by the largest deviation of any of these three other calculations from our preferred estimate. For the quantum calculations, the error estimate given is the largest deviation from our preferred estimate obtained using any of these three methods of interpolation combined with the logarithmic extrapolation near threshold or using any of the four methods of interpolation combined with the linear extrapolation near threshold.

E. Arrhenius Parameters. To calculate Arrhenius parameters each rate constant was calculated for eight evenly spaced values of $1/T$ in the range 0.003 33–0.001 K^{-1} (300 K ≤ T ≤ 1000 K) and the resulting rate constants were fit to the Arrhenius expression

$$k(T) = A \exp(-E_a/RT) \quad (10)$$

by adjusting A and E_a to minimize the sums of the squares of the differences of the calculated and fit values of log $k(T)$ at these eight temperatures. For this calculation we used a version of the program ACTEN[41] which was modified for the CYBER 74 computer.

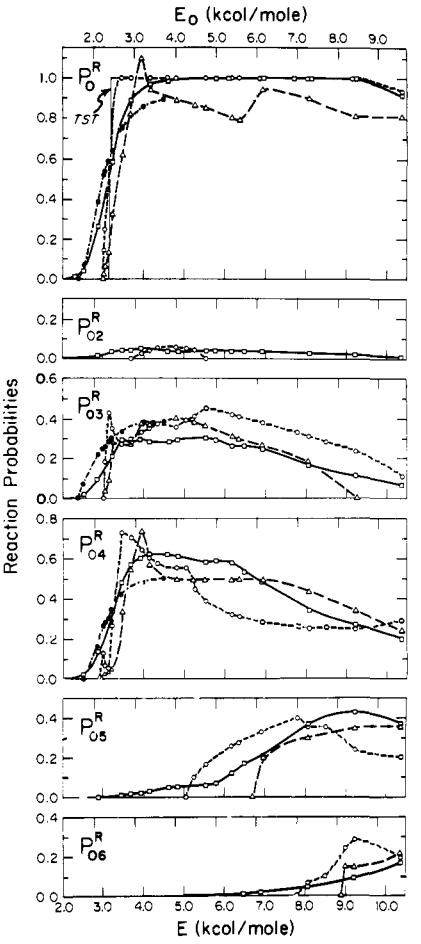

Figure 2. Comparison of the reaction probabilities P_0^R and $P_{0n_2}^R$ for the quantum (—), QCTH (- - -), and the BUSCCA (- -) calculations as functions of total energy e and initial relative kinetic energy E_0. QCTRH (- - -) calculations are shown only for P_0^R, P_{03}^R, and P_{04}^R. The TST reaction probability is also shown and is a step function with a threshold at total energy of 3.152 kcal/mol.

III. Results

A. State-to-State Reaction Probabilities and Fraction of Final Energy in Vibration. Figures 2–4 show the computed total and state-to-state reaction probabilities as functions of total energy E and translational energy E_{n_1} where

$$E_{n_1} = E - E_{n_1}^v(Cl_2) \quad (11)$$

At selected energies, Figures 5–7 show state-to-state reaction probabilities as functions of final vibrational quantum number. Since the BUSC approximation is the most generally applicable of the classical S matrix approximations the BUSCCA results are the only classical S matrix results shown in these figures. Numerical tables of all (quantum, QCTH, QCTRH, BUSCCA, AUSSCA, PSCCA, and CSCCA) the $P_{n_1 n_2}^R(E)$ and $P_{n_1}^R(E)$ values are given in the Appendix.[42]

Figure 8 shows the computed fractions $f_{n_1}(E)$ of total available energy (in excess of product zero-point energy) which is released as vibrational excitation energy of the product. This is computed as

$$f_{n_1}(E) = [P_{n_1}^R(E)]^{-1} \sum_{n_2} f(n_2, E) P_{n_1 n_2}^R(E) \quad (12)$$

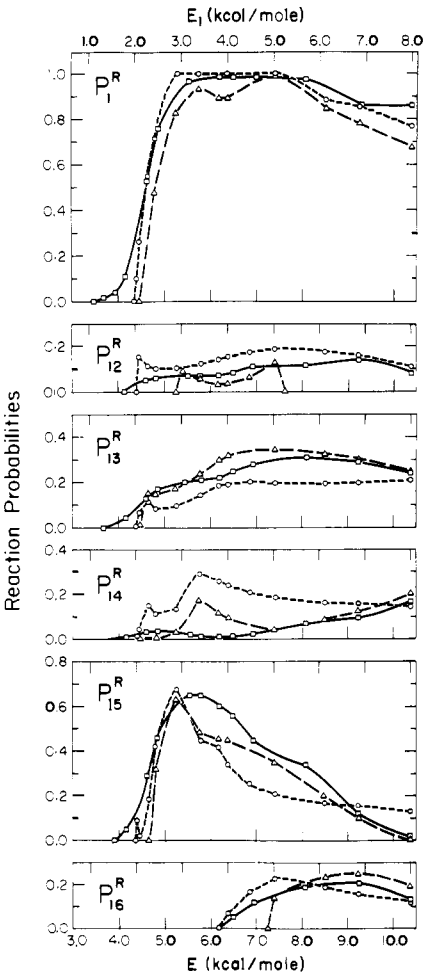

Figure 3. Reaction probabilities $P_1{}^R$ and $P_{1n_2}{}^R$ analogous to those given in Figure 1. E_1 is the initial relative kinetic energy. No QCRTH results are shown.

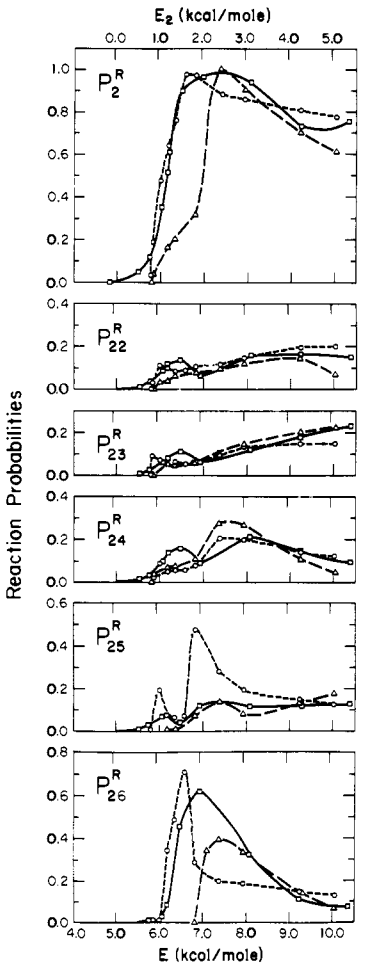

Figure 4. Reaction probabilities $P_2{}^R$ and $P_{2n_2}{}^R$ analogous to those given in Figure 1. E_2 is the initial relative kinetic energy. No QCRTH results are shown.

where

$$f(n_2,E) = \frac{E_{n_2}{}^v(\mathrm{HCl}) - E_0{}^v(\mathrm{HCl})}{E + \Delta E - E_0{}^v(\mathrm{HCl})} \quad (13)$$

where ΔE is the classical exothermicity. We also computed the average fraction of energy in product vibration for reaction of initial state with quantum number n_1 and translational temperature T as

$$f_{n_1}(T) = [k_{n_1}(T)]^{-1} \sum_{n_2} f[n_2,E_{n_1}{}^{\mathrm{avail}}(T)]k_{n_1n_2}(T) \quad (14)$$

where

$$E_{n_1}{}^{\mathrm{avail}}(T) = kT + E_a(n_1) \quad (15)$$

and $E_a(n_1)$ is the Arrhenius activation energy for k_{n_1}. Finally we computed the average fraction of energy in product vibration for reactant in a thermal system at temperature T as

$$f(T) = [k(T)]^{-1} \sum_{n_2} f[n_2,E^{\mathrm{avail}}(T)]k^{n_2}(T) \quad (16)$$

where

$$E^{\mathrm{avail}}(T) = kT + E_a \quad (17)$$

and E_a in this equation is the Arrhenius activation energy for the total rate constant k.

The $f_{n_1}(T)$ and $f(T)$ for the quantum, QCTH, and BUSSCA approximations are given in Table III.

B. Rate Constants. Figures 9–11 show the Arrhenius plots of state-to-state rate constants and total rate constants for a given initial state. Figure 12 shows the total rate constants computed for a thermal distribution of initial states. These are also tabulated in Table IV. The total rate constants into specific final states for a thermal distribution of initial states are given in Table V at selected temperatures.

Table III. The Average Fraction of Energy $f(T)$ in Product Vibration for Reactants in a Thermal System at Temperature T

	$f(T)$		
T, °K	Quantum	QCTH	BUSCCA
300	0.58	0.59	0.58
400	0.59	0.59	0.59
600	0.60	0.60	0.60
1000	0.61	0.61	0.61

Numerical tables of the quantum, QCTH, QCTRH, and BUSCCA values of $k_{n_1n_2}(T)$, $k_{n_1}(T)$, and $k^{n_2}(T)$ at eight evenly spaced temperatures in the range 300–1000 K are given in the Appendix.[42]

C. Arrhenius Parameters. Tables VI and VII give the Arrhenius parameters for the fits to the $k_{n_1n_2}(T)$, $k_{n_1}(T)$, and $k(T)$.

D. Transition-State Theory. For comparison purposes we also computed transition-state-theory one-dimensional rate constants using[43]

$$k^{\mathrm{TST}}(T) = (kT/h)[Q^{v\ddagger}(T)/Q^{\mathrm{rel}}(T)Q^v(T)] \times \exp(-E_0{}^{\mathrm{VAZC}}/kT) \quad (18)$$

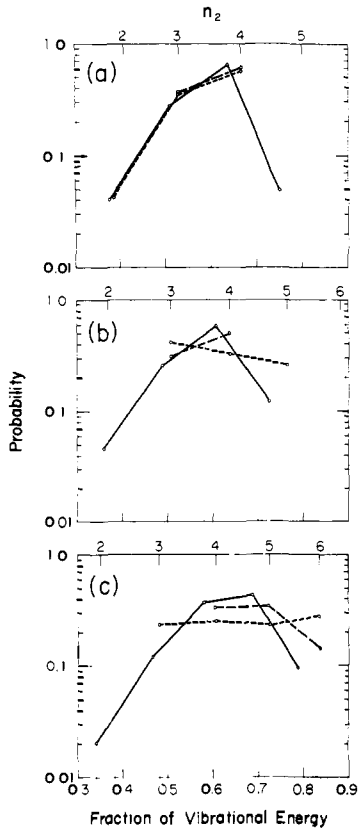

Figure 5. Distribution function of the final vibrational energy for the quantum (—), QCTH (- - -), and BUSCCA (- -) calculations for the ground vibrational state of reactant for total energies (a) 4.152 kcal/mol, (b) 6.181 kcal/mol, and (c) 9.225 kcal/mol. The upper abscissa scale represents the final vibrational quantum number.

Table IV. Comparison of the Quantum Thermal Rate Constant with Those Calculated Using the QCTH, BUSCCA, and TST Approximations

	$k(T)$				
T, °K	Quantum	QCTH	BUSCCA	$k^{TST}(T)$	$k^{TST/Q}(T)$
300	1.8 (3)[a]	1.21 (3)	8.58 (2)	1.23 (3)	1.89 (3)
400	4.8 (3)	3.76 (3)	2.81 (3)	3.85 (3)	4.72 (3)
500	9.0 (3)	7.59 (3)	5.83 (3)	7.85 (3)	8.75 (3)
600	1.4 (4)	1.22 (4)	9.55 (3)	1.28 (4)	1.37 (4)
700	1.9 (4)	1.72 (4)	1.36 (4)	1.85 (4)	1.92 (4)
800	2.4 (4)	2.22 (4)	1.77 (4)	2.45 (4)	2.52 (4)
900	2.8 (4)	2.70 (4)	2.17 (4)	3.07 (4)	3.13 (4)
1000	3.3 (4)	3.15 (4)	2.54 (4)	3.70 (4)	3.76 (4)

[a] The number in parentheses is the power of ten by which the entry should be multiplied. The units are cm molecule^{-1} s^{-1}.

where $Q^{v\ddagger}$ is a vibrational partition function calculated from the transition-state bound-normal-mode vibrational energies $E_n^{v\ddagger}$,[44] Q^{rel} is the relative-motion partition function per unit length, and E_0^{VAZC} is the ground-state vibrationally adiabatic barrier height (also called[43] the transition-state theory activation energy at 0 K). E_0^{VAZC} is given by

$$E_{n_1}^{VAZC} = E_b + E_{n_1}^{v\ddagger} - E_{n_1}^{v}(Cl_2) \qquad (19)$$

with $n_1 = 0$ and is 2.358 kcal/mol for the present calculations.

The above form of transition-state theory assumes the reaction coordinate is separable at the transition state, treats the reactant and the other degrees of freedom of the transition state quantum mechanically, and treats the reaction coordinate

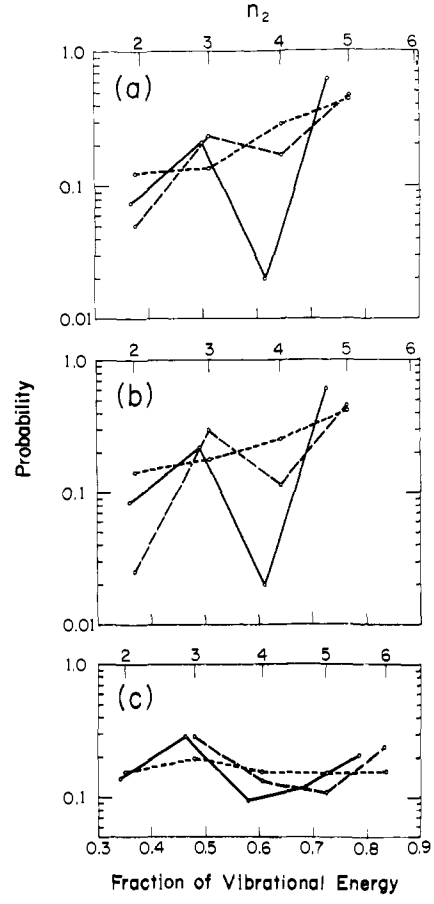

Figure 6. Distribution function of the final vibrational energy for the quantum (—), QCTH (- - -), and BUSCCA (- -) calculations for initial vibrational quantum number 1 for total energies (a) 5.765 kcal/mol, (b) 6.181 kcal/mol, and (c) 9.225 kcal/mol. The upper ordinate scale represents the final vibrational quantum number.

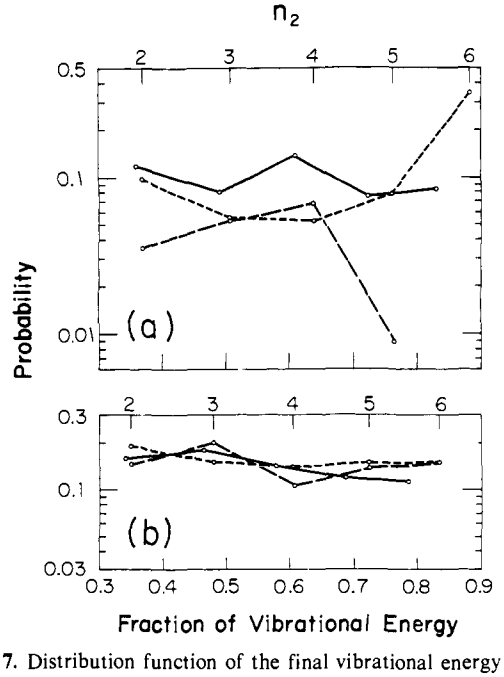

Figure 7. Distribution function of the final vibrational energy for the quantum (—), QCTH (- - -), and BUSCCA (- -) calculations for initial vibrational quantum number 2 for total energies (a) 6.181 kcal/mol and (b) 9.225 kcal/mol. The upper ordinate represents the final vibrational quantum number.

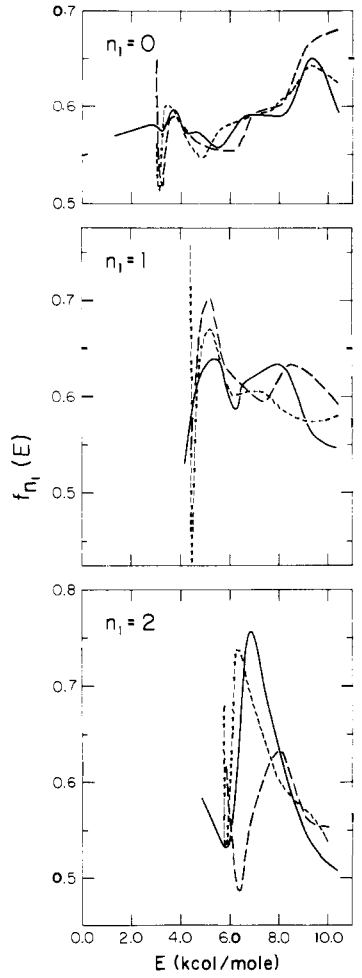

Figure 8. Fraction $f_{n_1}(E)$ of the total energy (in excess of product zero-point energy) which ends as vibrational excitation energy in the product HCl as a funtion of total energy for the quantum (—), QCTH (- - -), and BUSCCA (- -) calculations.

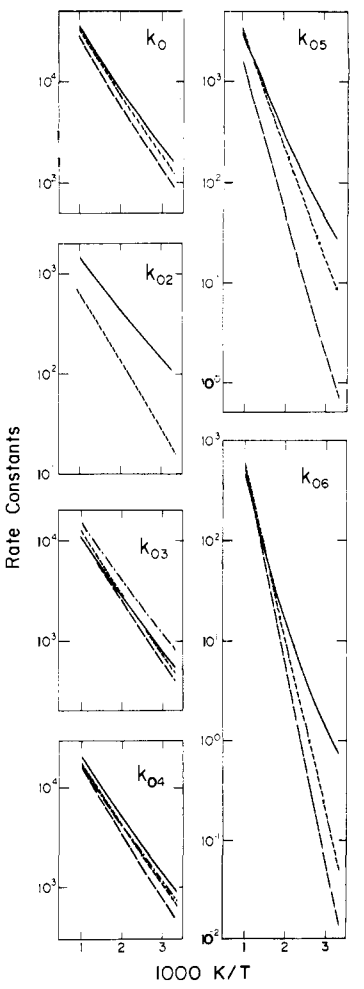

Figure 9. Quantum (—), QCTH (- - -), and BUSCCA (- -) rate constants k_0^R and $k_{0n_2}^R$ (cm/molecule·sec) as functions of reciprocal temperatures. QCTRH (- - -) results are shown only for k_{03}^R and k_{04}^R.

classically. We also evaluated the quantum correction on the reaction coordinate to lowest order in $\hbar$. This is[43,45]

$$\Gamma = 1 + (\hbar|\omega^{\ddagger}|/RT)^2/24 \qquad (20)$$

where $\omega^{\ddagger}$ is the imaginary frequency of the reaction-coordinate normal mode.[46] It yields the transition-state-theory rate constant corrected for tunneling (and nonclassical reflection) in the separable approximation as

$$k^{TST/Q}(T) = \Gamma k^{TST}(T) \qquad (21)$$

The transition-state theory rate constants are shown in Figure 12 and tabulated in Table IV.

The transition-state theory also predicts an average reaction probability as a function of total energy.[47] If one assumes that the transmission coefficient of transition-state theory is unity (which corresponds to assuming the reaction coordinate is separable at the transition state and the motion along the reaction coordinate is classical) the transition state theory reaction probability in the threshold energy region is a step function of step-height unity with a threshold at a total energy of $(E_0^{VAZC} + E_0^{v})$ which is 3.152 kcal/mol. This step function is shown at threshold in the top panel of Figure 2.

IV. Discussion

A. Total Reaction Probabilities, Total Rate Constants, and Arrhenius Parameters. The top panel of Figure 2 shows that there is very good agreement between the quantum and quasiclassical total reaction probabilities for ground-state reagents over the whole energy range. The major difference is the more gradual increase of the quantum results in the threshold region. This same type of behavior has been observed for the collinear $H + H_2$ reaction[7,8] and is most easily understood by analogy to a one-dimensional barrier problem where the quantum results show nonclassical tunneling at energies below the barrier height and nonclassical reflection at energies above it. It should be mentioned, however, that for the near-thermoneutral reaction $Cl + H_2$ and its isotopic analogues, the quasiclassical trajectory method seems to more systematically underestimate the reaction probability near threshold, at least for some of the isotopes.[15]

Figure 2 also shows that the calculation of the total reaction probability using the Bessel uniform semiclassical approximation of classical S matrix theory and the same trajectories as used for the quasiclassical trajectory calculations leads to reasonable results but nevertheless much worse results than the quasiclassical trajectory method.[48] Although the reaction threshold energy for the BUSCCA calculation is the same as that for the QCTH calculation in this case, the BUSCCA calculation predicts a much more slowly increasing reaction probability and is in much worse agreement with the quantum calculations near threshold. Thus the QCTH calculation is preferred over the BUSCCA calculation for the interpretation of the trajectories.[48]

The above conclusions are particularly interesting because they are almost diametrically opposed to the conclusions reached in the only other such studies[18-20] for an exothermic reaction. For $F + H_2$ and $F + D_2$, the uniform semiclassical

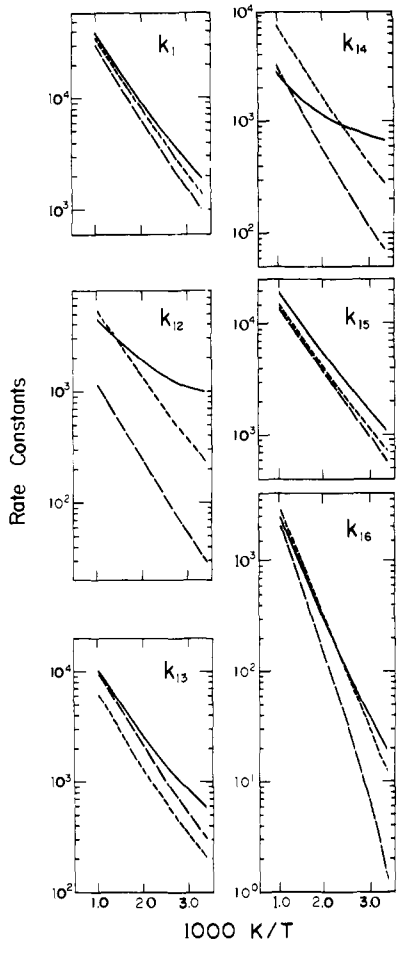

Figure 10. Rate constants k_1^R and $k_{1n_2}^R$ analogous to Figure 9.

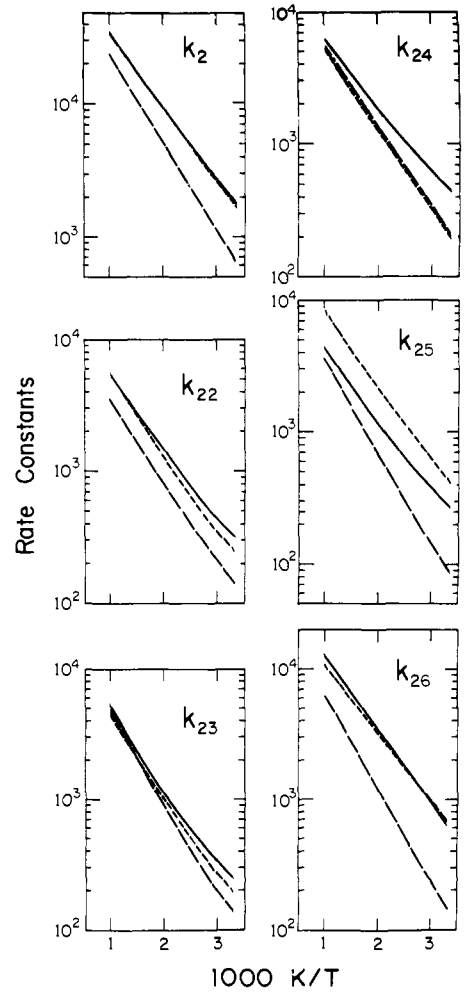

Figure 11. Rate constants k_2^R and k_{2n_2} analogous to Figure 9.

approximation using real-valued trajectories is much more accurate than the quasiclassical trajectory method using forward trajectories. Probably the two most important differences between the H + Cl_2 and F + H_2 cases are the masses and the higher potential energy barrier in the former case (for F + H_2 the classical barrier height on the surface used for the previous comparisons[18-20] is 1.06 kcal/mol[20]). However, further comparisons for other cases are needed to better understand the systematic errors of the trajectory calculations in the threshold regions.

It is also interesting to compare the effective threshold energies for reaction with each initial vibrational state. Table VIII compares these effective threshold energies. For all three initial vibrational states the results agree within 0.14 kcal/mol with the quantum results for the lowest energy at which the reaction probability is 0.5. However, the effective threshold energy is generally defined as a lower energy where the reaction probability is smaller. Figures 2-4 and Table VIII show that for such a definition the QCTH method more greatly overestimates the threshold energy, especially for the ground vibrational state of the reactant. Defining for discussion purposes the threshold energy as the energy where the reaction probability is 0.1, the QCTH method overestimates the threshold energies by 0.1-0.4 kcal/mol and the BUSCCA method predicts thresholds 0.1-0.2 kcal/mol higher than QCTH method except for the $n_1 = 2$ initial vibrational state where the QCTH method overestimates the threshold energy by only 0.1 kcal/mol but the BUSCCA method overestimates it by 1.0 kcal/mol.

It is interesting to see whether release of vibrational energy due to widening of the vibrational valley as the reactants proceed to the transition state is the main consideration for de-

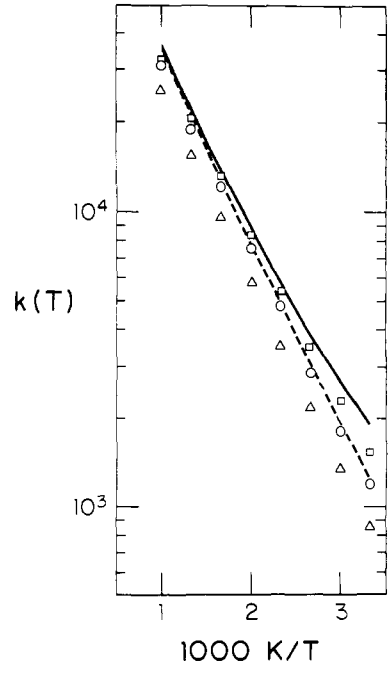

Figure 12. Comparison of the quantum (□), QCTH (○), and BUSCCA (△) rate constants (cm/(molecule·s)) averaged over thermal distributions of reactant vibrational states and summed over final vibrational states to the transition state rate constants k^{TST} (- - -) and $k^{TST/Q}$ (—) as functions of reciprocal temperatures.

Table V. Comparison of Quantum, QCTH, and BUSCCA Thermally Averaged Rate Constants $k^{n_2}(T)$ for Production of Specific Final States n_2 at Selected Temperatures

T, °K		n_2 = 2	3	4	5	6
300	Quantum	1.66 (2)[a]	5.39 (2)	9.74 (2)	9.91 (1)	5.13 (0)
600		1.04 (3)	3.87 (3)	6.35 (3)	2.11 (3)	4.18 (2)
1000		2.55 (3)	8.60 (3)	1.26 (4)	6.80 (3)	2.18 (3)
300	QCTH	3.11 (1)	4.59 (2)	6.50 (2)	5.65 (1)	4.27 (0)
600		6.63 (2)	3.86 (3)	5.51 (3)	1.74 (3)	3.95 (2)
1000		2.26 (3)	8.82 (3)	1.18 (4)	6.19 (3)	2.18 (3)
300	BUSCCA	1.90 (0)	3.71 (2)	4.44 (2)	3.85 (1)	9.16 (−1)
600		1.48 (2)	3.61 (3)	4.38 (3)	1.26 (3)	1.92 (2)
1000		6.75 (2)	8.62 (3)	1.02 (4)	4.65 (3)	1.52 (3)

[a] The number in parentheses is the power of ten by which the entry should be multiplied. The units are cm molecule^{-1} s^{-1}.

Table VI. Arrhenius Rate Constant Parameters for $k_{n_1 n_2}(T)$ for the Temperature Range 300–1000 K[a]

		Quantum		QCTH		QCTRH		BUSCCA	
n_1	n_2	A	E_a	A	E_a	A	E_a	A	E_a
0	2	4.21 (3)[b]	2.22	3.16 (3)	3.16	n.c.[c]	n.c.	c.f.[d]	c.f.
0	3	3.51 (4)	2.52	4.88 (4)	2.78	4.90 (4)	2.46	4.37 (4)	2.85
0	4	7.24 (4)	2.58	6.79 (4)	2.75	5.79 (4)	2.61	7.00 (4)	3.00
0	5	1.86 (4)	4.00	4.08 (4)	5.13	n.c.	n.c.	4.01 (4)	6.56
0	6	4.82 (4)	5.49	3.09 (4)	7.97	n.c.	n.c.	4.77 (4)	9.00
1	2	7.57 (3)	1.31	1.87 (4)	2.64	n.c.	n.c.	5.72 (3)	3.19
1	3	2.88 (4)	2.38	2.29 (4)	2.87	n.c.	n.c.	3.77 (4)	2.90
1	4	3.95 (3)	1.15	2.79 (4)	2.78	n.c.	n.c.	1.46 (4)	3.21
1	5	6.28 (4)	2.43	5.09 (4)	2.55	n.c.	n.c.	5.57 (4)	2.75
1	6	1.69 (4)	4.10	2.59 (4)	4.53	n.c.	n.c.	3.25 (4)	5.56
2	2	1.68 (4)	2.41	1.93 (4)	2.65	n.c.	n.c.	1.33 (4)	2.73
2	3	1.67 (4)	2.59	1.53 (4)	2.67	n.c.	n.c.	1.97 (4)	3.03
2	4	1.73 (4)	2.22	2.00 (4)	2.76	n.c.	n.c.	2.10 (4)	2.76
2	5	1.30 (4)	2.34	2.87 (4)	2.54	n.c.	n.c.	1.63 (4)	3.15
2	6	4.58 (4)	2.56	3.43 (4)	2.34	n.c.	n.c.	3.13 (4)	3.20

[a] A and E_a have units of cm molecule^{-1} s^{-1} and kcal/mol, respectively. [b] The number in parentheses is the power of ten by which the entry should be multiplied. [c] n.c.: these rate constants were not calculated. [d] c.f.: this transition is classically forbidden so the BUSCCA rate constant is identically zero.

Table VII. Arrhenius Rate Constant Parameters for $k_{n_1}(T)$ and $k(T)$ for the Temperature 300–1000 K[a]

	Quantum		QCTH		BUSCCA	
n_1	A	E_a	A	E_a	A	E_a
0	1.28 (5)[b]	2.68	1.38 (5)	2.86	1.22 (5)	2.99
1	1.26 (5)	2.54	1.34 (5)	2.73	1.24 (5)	2.90
2	1.14 (5)	2.48	1.19 (5)	2.54	9.05 (4)	3.02
	1.19 (5)	2.61	1.27 (5)	2.79	1.09 (5)	2.90

[a] A and E_a have units of cm molecule^{-1} s^{-1} and kcal/mol, respectively. [b] The number in parentheses is the power of ten by which the entry should be multiplied.

termining the differences in the threshold energies. Since the barrier occurs early we might expect the motion between the reagent configuration and the transition state one to be vibrationally adiabatic.[49-51] We will use the vibrationally adiabatic zero-curvature model[52] to study this question. In this model one expects the reaction probability to be about 0.5 at a translational energy equal to the VAZC barrier height defined in eq 19. The comparison of this theory with the quantum calculations is given in Table VIII. It shows that the VAZC theory predicts the threshold energy within 0.11 kcal/mol. This is very good, in accord with our expectations based on previous applications to reactions with symmetric barriers.[12,52]

The top panels of Figures 3 and 4 show that the main features of the comparison of quantum, QCTH, and BUSCCA total reaction probabilities as functions of energy are the same for excited reagents as for ground state ones. In particular, the QCTH results are still in good agreement with the quantum ones over the whole energy range although they show a more rapid increase with energy in the threshold region. But, as mentioned already, the BUSCCA results are much too small or zero in the threshold region. Further they are not quite as accurate as the QCTH results are at higher energies.

The differences in the reaction probabilities discussed above have direct consequences for the total rate constants for selected initial states given in the Appendix and Figures 9–11. At higher temperatures the QCTH rate constants are very accurate (at 1000 K they agree with the quantum results within the estimates of possible numerical error for all three initial vibrational states) while the errors in the BUSCCA rate constants are a little larger. At lower temperatures for n_1 equals 0 and 1 the QCTH results fall a little below the quantum ones (22–29% at 300 K) while the BUSCCA results have much larger errors (too low by about a factor of 2). The good agreement of the QCTH results with the quantum ones over the whole temperature range for n_1 equals 2 is most impressive.

The temperature dependence and direction of these errors in the rate constants are easily understood in terms of the low-energy tail of the quantum probability of reaction. The

Table VIII. Comparison of the Relative Translational Energies $E_{n_1}^{x}$ (kcal/mol) at which the Reaction Probabilities $P_{n_1}^{R}$ for Initial State n_1 become x with the Vibrationally Adiabatic Zero-Curvature Barrier Heights $E_{n_1}^{VAZC}$ (also in kcal/mol) for Initial State n_1

	$E_{n_1}^{0.1}$			$E_{n_1}^{0.5}$			
n_1	BUSCCA	QCTH	Quantum	BUSCCA	QCTH	Quantum	$E_{n_1}^{VAZC}$
0	2.32	2.23	1.83	2.58	2.37	2.35	2.37
1	2.14	2.03	1.82	2.46	2.25	2.21	2.25
2	2.08	1.89	1.79	3.0	2.11	2.25	2.14

Table IX. Maximum Values of $P_{n_1n_2}^{R}$ for $E \leq 10.38$ kcal/mol[a]

		$P_{n_1n_2}^{R}$		
n_1	n_2	Quantum	QCTH	BUSCCA
0	2	0.04	0.05	0.00
	3	0.30	0.44	0.40
	4	0.62	0.73	0.74
	5	0.43	0.40	0.36
	6	0.17	0.28	0.21
	7	n.a.[b]	0.12	0.00
1	2	0.14	0.18	0.13
	3	0.31	0.21	0.34
	4	0.10	0.29	0.21
	5	0.65	0.68	0.62
	6	0.21	0.23	0.25
	7	n.a.[b]	0.06	0.00
2	2	0.16	0.20	0.15
	3	0.23	0.15	0.22
	4	0.20	0.21	0.28
	5	0.13	0.48	0.19
	6	0.62	0.49	0.39
	7	n.a.[b]	0.03	0.00

[a] These numbers are only lower bounds since the searches for maxima were not carried out to an accuracy of 0.01. [b] Not available.

various calculations disagree most strongly in the energy region of this tail and this region makes the most important fractional contribution to the rate constant at low temperatures. Thus Table VII shows that the BUSCCA and QCTH methods overestimate the energy of activation by 0.29 and 0.18 kcal/mol, respectively. The agreement of the QCTH Arrhenius energy of activation with the quantum one within 0.2 kcal/mol is very encouraging for practical applications of the QCTH method. For example a quasiclassical trajectory calculation of the Arrhenius energy of activation has sometimes been used[51] for the determination of parameters in semiempirical potential energy surfaces. While such a procedure is obviously incapable of uniquely determining a potential energy surface, it is encouraging that it is not shown to lead to large systematic errors.

The top panel of Figure 2 shows that the average reaction probability computed from transition-state theory (TST) with the classical approximation for motion along the reaction coordinate agrees with the quasiclassical trajectory calculation very well and thus is also in good agreement with the quantum calculations. Because of the very good agreement of the TST and QCTH average reaction probabilities, it is not surprising that the rate constants (see Table IV and Figure 12) are also in good agreement. As expected the disagreement of TST rate constants with the QCTH and quantum results is greatest at low temperatures where the calculated rate constant is most sensitive to the details of the threshold reaction probabilities. Thus the TST rate constant differs from the quantum one by 20% at 300 K but by only 13% at 1000 K. Since the TST rate constant is too low at low temperatures, a quantum treatment of the reaction coordinate might be expected to provide an improved result. However, Table IV and Figure 12 show that the Wigner "tunneling correction" is too large to improve the comparison with the quantum results. This might have been expected since it is known that quantum corrections to a separable reaction coordinate are inaccurate for the collinear H + H_2 reaction.[53] Miller and co-workers have shown that nonseparable transition state theory treatments are much more accurate in that case.[54]

B. State-to-State Reaction Probabilities, Rate Constants, and Arrhenius Parameters. Ground-State Reagents. Figures 2 and 5 show good general agreement of the QCTH and BUSCCA methods for the magnitudes of the state-to-state reaction probabilities $P_{0n_2}^{R}$ except in the threshold region, where they underestimate the reaction probability. This good agreement is illustrated for example by the maximum values obtained for each probability at any energy. These are compared in Table IX. The agreement of the various $P_{n_1n_2}^{R}$ curves is best for n_2 equals 3 and 4 and worst for n_2 equals 2 and 7. This is not surprising since the histogram method should not be expected to be accurate for the lowest and highest vibrational states for which it predicts nonzero values and since complex-valued trajectories should be important for these states in classical S matrix theory. Although reaction into the $n_2 = 2$ state is actually classically forbidden, the QCTH method leads to nonzero P_{02}^{R} in the energy range 3.7–5.5 kcal/mol. The QCTRH method predicts a zero value of P_{02}^{R} up to an energy of 5.25 kcal/mol. The poor agreement of the QCTH and quantum results for n_2 equals 4 at the relatively high total energies around 6 kcal/mol is much more surprising. The extremely wide threshold region for n_2 equals 5 also causes considerable error. In all cases the BUSCCA method is inaccurate near threshold. The QCTH method leads to quite complicated threshold behavior for n_2 equals 4 and in this case the reverse quasiclassical trajectory method is much more accurate. For n_2 equals 3 the reverse quasiclassical trajectory method again leads to a more accurate threshold value and a more qualitatively correct dependence on energy in the threshold region. But it overestimates P_{03}^{R} over the whole energy region (up to 4.5 kcal/mol) for which it was calculated and the rate constant is not improved as discussed in the next paragraph.

Figure 2 shows that only P_{03}^{R} and P_{04}^{R} contribute significantly to the reaction probability for energies up to about 8 kcal/mol where P_{05}^{R} begins to contribute significantly. Thus the good agreement of the QCTH and quantum values for P_{03}^{R} and P_{04}^{R} discussed just above ensure the good agreement of the QCTH and quantum values of the rate constants as shown in the top panel of Figure 9 and discussed in the previous subsection. Figure 9 also shows that the errors in the QCTH state-to-state rate constants are smallest for the largest rate constants; thus the errors are less than or equal to 23 and 32% over the whole temperature range for the QCTH method for n_2 equals 3 and 4, respectively. But the large error in the threshold region causes errors of factors of 3.5 and 39 for the QCTH and BUSCCA rate constants, respectively, for n_2 equal to 5 at 300 K. Even for this case, however, the errors are considerably smaller at higher temperatures. The reverse quasiclassical trajectory method leads to more accurate rate con-

stants than the forward method for $n_2 = 4$ at low enough temperature but is otherwise less accurate for state-to-state rate constants. The QCTH rate constant for $n_2 = 2$ is in poor agreement with the quantum rate constant at all temperatures; this could have been expected since this transition is classically forbidden. At low temperatures the threshold energy region contributes significantly to the rate constants and the QCTH and BUSCCA methods systematically underestimate all the state-to-state rate constants due to reactive thresholds being at higher energies than the corresponding quantum ones. Interestingly, the incorrect threshold behavior of the QCTRH method for $P_{03}{}^R$ (see Figure 2) results in an overestimate of the rate constant $k_{03}(T)$ at all temperatures.

The Arrhenius activation energies for the state-to-state rate constants are affected in a predictable manner. Table VI shows that the activation energies computed from the quantum rates are always lower than the QCTH and BUSCCA values for $n_1 = 0$. For k_{03} and k_{04}, however, the QCTRH method predicts lower activation energies than the quantum ones. These results are all in agreement with the discussion of the state-to-state reaction probabilities earlier in this section.

Excited Reactants. Figures 3 and 4 and Tables VIII and IX show that the trajectory calculations are in many cases even more accurate for excited reactants than for ground state ones but there are some interesting exceptions (notably $P_{12}{}^R$, $P_{14}{}^R$, $P_{25}{}^R$, and $P_{26}{}^R$). Consider first n_1 equals 1. The QCTH results for $P_{12}{}^R$ near threshold and $P_{14}{}^R$ throughout the whole energy region are in very poor agreement with the quantum results. The QCTH results for $P_{13}{}^R$, $P_{15}{}^R$, and $P_{16}{}^R$ are in good qualitative agreement with the quantum calculations although near threshold the QCTH results for $P_{13}{}^R$ and $P_{15}{}^R$ are too small. This effect is similar, for example, to what was seen for $P_{03}{}^R$. The BUSCCA calculations are in good agreement with the quantum ones for reactive transitions which are strongly classically allowed. In the threshold energy regions we again find that the BUSCCA approximation severely underestimates the state-to-state reaction probabilities. For n_1 equals 1, the reverse quasiclassical trajectory method again seems to improve the threshold values of the various state-to-state reaction probabilities.

For n_1 equals 2, the QCTH and BUSCCA state-to-state reaction probabilities are in very good agreement with the quantum ones, except for $P_{25}{}^R$ and $P_{26}{}^R$. For these two transitions the QCTH method predicts an incorrect dependence on energy and the BUSCCA method leads to thresholds about 1 kcal/mol too high. The delayed threshold for $P_{26}{}^R$ dramatically affects the BUSCCA curve for $P_2{}^R$ and may be considered responsible for its gross disagreement with the quantum results (see top panel of Figure 4).

The good general agreement of the QCTH and BUSCCA state-to-state reaction probabilities with the quantum ones is illustrated more clearly at selected energies in Figures 6 and 7. Again we see that for weakly classically allowed processes (i.e., cases where the QCTH state-to-state reaction probabilities are small and the BUSCCA ones are nonzero) the QCTH and BUSCCA results are not reliable, while for cases where the process is more strongly classically allowed the QCTH and BUSCCA results are in better agreement with the quantum results. It should be pointed out that the quantum results in Figures 5–7 are plotted using Baer's incorrect values for the vibrational energies. It is seen that the agreement with the present results would be improved if they were plotted at the correct energies. This may indicate that the associated inaccuracies in the quantum results may not be large.

Figures 10 and 11 again show that the rate constants computed from the trajectory calculations are in good agreement with the quantum ones at large temperatures with a few notable exceptions. Although more state-to-state rate constants are large for excited reactants, the errors in the quasiclassical results have not become uniformly smaller than for ground state reactants. There are errors of about a factor of 2 or even a little larger over the whole temperature range for three of the fairly large state-to-state rate constants, namely, for the $1 \rightarrow 3$, $1 \rightarrow 4$, and $2 \rightarrow 5$ processes. These results serve as a caution that the quasiclassical trajectory histogram method is sometimes unreliable even for results for classically allowed processes averaged over a translational energy distribution corresponding to a temperature as high as 1000 K. The errors in these three rate constants are in each case due to a systematic error (underestimates or overestimates) in the state-to-state reaction probabilities over the whole important energy region.

At lower temperatures the QCTH and BUSCCA methods underestimate the rate constants for all cases except the QCTH results for k_{25} and k_{26}. This general result is due to the thresholds being generally too high in the trajectory methods.

Just as for the ground states, Table VI shows the Arrhenius activation energies are generally fairly accurate when the quantum value for the preexponential factor A exceeds 10^4 molecules/(cm s).

Overall the BUSCCA method is less accurate than the QCTH method for excited reactants.

Summary. Although the quasiclassical trajectory method is accurate within 29% for the overall rate constant out of any vibrational state of Cl_2 over the whole temperature range, the state-to-state rate constants determined by the histogram procedure are less accurate and in some cases are much less accurate (in error by a factor of 2 or larger) even for classically allowed transitions. The errors in the quasiclassical trajectory rate constants are mostly due to errors in the threshold region but in some cases there are quite significant errors due to higher energy failures of the histogram method. In general the errors are less serious for the Arrhenius activation energies. The classical **S** matrix theory does not provide a generally better method for extracting state-to-state transition probabilities from these (real-valued) trajectory calculations.

It is interesting to compare the results of the present study to those of Schatz et al. For $F + H_2$ and $F + D_2$ it was found that the QCTRH and BUSCCA methods were in much better agreement with the quantum mechanical calculations than the QCTH method. The present study shows that the QCTH method is in better agreement with the quantum results than the QCTRH and BUSCCA are (except right near threshold where the QCTRH method appears to be more accurate). Thus, one should be cautious in selecting a preferred method for interpreting quasiclassical trajectories or making generalizations concerning the applicability or accuracy of the various methods.

C. Percentage of Energy Released in Vibration. Figure 8 shows that generally the fraction of available energy predicted to be in vibration by the QCTH and BUSCCA methods is in reasonably good agreement with the quantum results. There are, however, important differences near threshold. Due to the long history of applying quasiclassical trajectory calculations to predict the vibrational energy of products of thermal reactions, there is considerable interest in the threshold energy region of these curves for ground-state reactants. Thus it is notable that the QCTH results in that case differ from the quantum ones in a qualitatively different way than in the only previous available comparison.[18,19] Thus one must be very cautious about generalizing the shapes of these curves and the directions of the errors to other cases.

Table II shows that, on averaging over thermal distributions of translational energy, the fraction of energy predicted to be in product vibration by either the QCTH or BUSCCA method is in *excellent* agreement with the quantum calculations for all temperatures for n_1 equals 0. Thus the results further av-

eraged over a thermal distribution of vibrational states (Table III) are also excellent. For excited reactants, the agreement with quantum results (Table II) is again good at higher temperatures but the trajectory results are in error by as much as about 10% at 300 K.

V. Concluding Remarks

The quasiclassical trajectory histogram method has been tested against exact quantum mechanical calculations for state-to-state reaction probabilities for the collinear reaction $H + Cl_2$. This method uses classical trajectories corresponding to the correct quantized initial vibrational action variables and uses the histogram method to assign final vibrational quantum numbers. We also examined the use of classical S matrix theory to assign final vibrational quantum numbers. Although other methods of assigning final vibrational quantum numbers are possible[55] they were not tried. Particular care was taken to evaluate the histogram results precisely so that conclusions based on comparison to exact quantum results are the correct conclusions about the classical approximations, i.e., about real errors in the method as opposed to statistical (Monte Carlo) errors. We find the errors in trajectory calculations are largest near threshold and are larger for vibrationally excited states of the reactants than for ground state reactants. Errors are smaller but not always insignificant when results are averaged over thermal distributions of reactant states. Since trajectory calculations are widely used to compute product vibrational energy or state distributions, the results in Tables II, III, and V are particularly interesting. They show, for example, that for ground-state reactants with a thermal distribution of relative translational energies, the average vibrational energy of the products can be accurately predicted at either 1000 or 300 K and the trajectory results for the complete distribution of state-to-state reaction probabilities are accurate at 1000 K, but the latter are not accurate at 300 K.

Acknowledgment. This work was supported in part by the National Science Foundation. We are grateful to Dr. Michael Baer for preprints of ref 15 and 22 and for sending some of his results in tabular form.

Supplementary Material Available: State-to-state reaction probabilities and rate constants, total reaction probabilities and rate constants out of given initial states, and thermally averaged rate constants into specific final states in Tables A-1-A-9 (17 pages). Ordering information is given on any current masthead page.

References and Notes

(1) (a) Alfred P. Sloan Foundation Research Fellow, 1973-present; Joint Institute for Laboratory Astrophysics Visiting Fellow, 1975-1976; (b) National Science Foundation Undergraduate Research Participant, 1974; (c) National Defense Education Act Fellow, 1971-1974.
(2) R. N. Porter, *Annu. Rev. Phys. Chem.*, **25**, 317 (1974).
(3) M. Karplus, R. N. Porter, and R. D. Sharma, *J. Chem. Phys.*, **43**, 3259 (1965).
(4) R. D. Levine and R. B. Bernstein, "Molecular Reaction Dynamics", Oxford University Press, New York, N.Y., 1974, pp 154 and 155.
(5) A. Kuppermann and G. C. Schatz, *J. Chem. Phys.*, **62**, 2502 (1975); A. B. Elkowitz and R. E. Wyatt, *ibid.*, **62**, 2504 (1975); J. D. Doll, T. F. George, and W. H. Miller, *ibid.*, **58**, 1343 (1973).
(6) A. Altenberger-Siczek and J. C. Light, *J. Chem. Phys.*, **61**, 4373 (1974).
(7) E. M. Mortensen, *J. Chem. Phys.*, **49**, 3526 (1969); D. J. Diestler and M. Karplus, *ibid.*, **55**, 5832 (1971).
(8) J. M. Bowman and A. Kuppermann, *Chem. Phys. Lett.*, **12**, 1 (1972).
(9) K. P. Fong and D. J. Diestler, *J. Chem. Phys.*, **56**, 3200 (1972).
(10) J. M. Bowman and A. Kuppermann, *Chem. Phys. Lett.*, **19**, 166 (1973).
(11) J. M. Bowman and A. Kuppermann, *J. Chem. Phys.*, **59**, 6524 (1973).
(12) J. W. Duff and D. G. Truhlar, *Chem. Phys. Lett.*, **23**, 327 (1973).
(13) J. W. Duff and D. G. Truhlar, *Chem. Phys.*, **4**, 1 (1974).
(14) (a) A comparison of exact quantum and quasiclassical results in a time-dependent framework is given by E. A. McCullough, Jr., and R. E. Wyatt, *J. Chem. Phys.*, **51**, 1253 (1969); **54**, 3578, 3592 (1971); (b) a review of comparisons of trajectory methods and accurate quantum calculations for $H + H_2$ is given by D. G. Truhlar and R. E. Wyatt, *Annu. Rev. Phys. Chem.*, **27**, in press.
(15) M. Baer, U. Halavee, and A. Persky, *J. Chem. Phys.*, **61**, 5122 (1974).
(16) G. C. Schatz, J. M. Bowman, and A. Kuppermann, *J. Chem. Phys.*, **58**, 4023 (1973).
(17) J. M. Bowman, G. C. Schatz, and A. Kuppermann, *Chem. Phys. Lett.*, **24**, 378 (1974).
(18) G. C. Schatz, J. M. Bowman, and A. Kuppermann, *J. Chem. Phys.*, **63**, 674 (1975).
(19) G. C. Schatz, J. M. Bowman, and A. Kuppermann, *J. Chem. Phys.*, **63**, 685 (1975).
(20) P. A. Whitlock and J. T. Muckerman, *J. Chem. Phys.*, **61**, 4618 (1974).
(21) D. Russell and J. C. Light, *J. Chem. Phys.*, **51**, 1720 (1969).
(22) M. Baer, *J. Chem. Phys.*, **60**, 1057 (1974).
(23) W. H. Miller, *Adv. Chem. Phys.*, **25**, 69 (1974); **30**, 77 (1975).
(24) T. F. George and W. H. Miller, *J. Chem. Phys.*, **56**, 5722 (1972); **57**, 2458 (1972); J. D. Doll, T. F. George, and W. H. Miller, *ibid.*, **58**, 1343 (1973); S. M. Hornstein and W. H. Miller, *ibid.*, **61**, 745 (1974).
(25) S.-F. Wu and R. D. Levine, *Mol. Phys.*, **25**, 937 (1973). The quantum results used for this comparison were subsequently shown to be inaccurate; see, e.g., S. Wu, B. R. Johnson, and R. D. Levine, *Mol. Phys.*, **25**, 609 (1973); J. W. Duff and D. G. Truhlar, *Chem. Phys. Lett.*, **23**, 327 (1973).
(26) C. C. Rankin and W. H. Miller, *J. Chem. Phys.*, **55**, 3150 (1971).
(27) Comprehensive sets of references to previous work are given by N. C. Blais and D. G. Truhlar, *J. Chem. Phys.*, **61**, 4186 (1974); D. L. Thompson, H. H. Suzukawa, Jr., and L. M. Raff, *ibid.*, **62**, 4727 (1975); and R. L. Wilkins, *ibid.*, **63**, 2963 (1975).
(28) P. J. Kuntz, E. M. Nemeth, J. C. Polanyi, S. D. Rosner, and C. E. Young, *J. Chem. Phys.*, **44**, 1168 (1966).
(29) C. A. Parr, J. C. Polanyi, and W. H. Wong, *J. Chem. Phys.*, **58**, 5 (1973).
(30) J. D. McDonald, P. R. LeBreton, Y. T. Lee, and D. R. Herschbach, *J. Chem. Phys.*, **56**, 769 (1972).
(31) Following a common convention we call trajectories quasiclassical if the diatomic starts the trajectory with one of its quantized vibrational energies.
(32) W. H. Miller, *J. Chem. Phys.*, **53**, 3578 (1970).
(33) J. R. Stine and R. A. Marcus, *J. Chem. Phys.*, **59**, 5145 (1973).
(34) J. W. Duff and D. G. Truhlar, *Chem. Phys.*, **9**, 243 (1975).
(35) L. Gottdiener, *Mol. Phys.*, **29**, 1585 (1975).
(36) J. N. L. Connor, *Mol. Phys.*, **26**, 1217 (1973).
(37) J. N. L. Connor, *Mol. Phys.*, **27**, 853 (1974).
(38) J. R. Stine and R. A. Marcus, *Chem. Phys. Lett.*, **29**, 575 (1974).
(39) D. G. Truhlar and A. Kuppermann, *J. Chem. Phys.*, **56**, 2232 (1972).
(40) M. Baer, private communication.
(41) Available as program No. 179 from Quantum Chemistry Program Exchange, Chemistry Department, Indiana University, Bloomington, Ind. 47401.
(42) The Appendix consists of Tables A-1-A-9. It is available in the microfilm edition of this journal; it is also available separately (consult the masthead page for ordering information).
(43) H. S. Johnston, "Gas Phase Reaction-Rate Theory", Ronald Press, New York, N.Y., 1966; D. Rapp, "Statistical Mechanics", Holt, Rinehart and Winston, New York, N.Y., 1972.
(44) These were approximated using the Morse approximation as $E_n^{v\ddagger} = [1.487(n + \frac{1}{2}) - 0.011\,96(n + \frac{1}{2})^2]$ kcal/mol.
(45) E. Wigner, *Z. Phys. Chem., Abt. B*, **19**, 203 (1932).
(46) For the present potential energy surface and masses, $h\omega^{\ddagger} = 1.394i$ kcal/mol.
(47) K. Morokuma, B. C. Eu, and M. Karplus, *J. Chem. Phys.*, **51**, 5193 (1969).
(48) The reader should note that throughout this article we compare the usefulness of the QCTH, QCTRH, and BUSCCA methods for calculating quantumlike probabilities from a batch of real-valued classical trajectories. This is one important question. Related questions concerning the usefulness of the BUSC approximation when complex-values root trajectories are calculated and the accuracy of classical **S** matrix theory when more accurate uniform approximations, which have not yet been shown to exist or developed, are used are not addressed in the present article.
(49) R. A. Marcus, *J. Chem. Phys.*, **45**, 4493, 4500 (1966).
(50) J. C. Polanyi and W. H. Wong, *J. Chem. Phys.*, **51**, 151 (1969).
(51) N. C. Blais and D. G. Truhlar, *J. Chem. Phys.*, **58**, 1090 (1973).
(52) D. G. Truhlar, A. Kuppermann, and J. T. Adams, *J. Chem. Phys.*, **59**, 395 (1973), and references therein.
(53) D. G. Truhlar and A. Kuppermann, *Chem. Phys. Lett.*, **9**, 269 (1971).
(54) S. Chapman, B. C. Garrett, and W. H. Miller, *J. Chem. Phys.*, **63**, 2710 (1975).
(55) D. G. Truhlar, *Int. J. Quantum Chem., Symp.*, **10**, in press.